

UDC 669.715:672.791

MICROSTRUCTURE AND MECHANICAL PROPERTIES OF WELDED JOINTS OF ALUMINUM ALLOY AA7020-T6 OBTAINED BY FRICTION STIR WELDING

G. Srinivasa Rao,¹ V. V. Subba Rao,² and S. R. K. Rao³

Translated from *Metallovedenie i Termicheskaya Obrabotka Metallov*, No. 3, pp. 8 – 13, March, 2017.

Plates from alloy AA7020 (Al – Zn – Mg) with a thickness of 4.5 mm are studied after T6 heat treatment and friction stir welding. Tensile and bending tests are performed. The hardness of the welds is measured in transverse direction. The microstructure over cross section of a weld is studied by the methods of light and transmission electron microscopy. The weldability of alloy AA7020 by friction stir welding is shown to be high.

Key words: aluminum alloys, friction stir welding, microstructure, transmission electron microscopy.

INTRODUCTION

Alloy AA7020 of the Al – Zn – Mg system has a moderate strength and is used widely in welded joints of bridge beams, road and railroad systems, armored vehicles, cryogenic pressure vessels and components of spacecraft liquid-propellant engines [1, 2]. Some characteristic defects arise in mechanisms obtained by fusion welding. It is reported in [3, 4] that cracks appear in different stages of post-welding mechanical treatment and assemblage in argon-arc-welded joints. They are caused by residual stresses present in the material. Alloy AA7020 is well weldable by fusion, but its mechanical properties vary considerably due to dissolution of the hardening precipitates in the fusion zone [5, 6]. In addition, such alloys are susceptible to hot cracking if not subjected to a special treatment. A way to lower hot cracking is refinement of grains in the fusion zone [7] by introducing inoculating additions during the fusion welding or choosing another type of welding not requiring a filler. Cracking has also been observed under solidification of electron-beam-welded Al – Zn – Mg alloys without filler [8]. The recently published results of the studies of microstructure and mechanical properties of aluminum alloy 7020 after electron-beam welding [9] have shown considerable lowering of

the hardness and ductility in the fused zone. Refinement of microstructure due to inoculation and its effect on hot cracking and on the properties of a welded joint of alloy 7020 under tensile testing has been studied in [10]. In the tensile tests, the hot cracking was reduced and the properties of the alloy improved. However, the gain in the ductility was not considerable. On the whole, fusion welding of alloys of the Al – Zn – Mg system is characterized by such flaws as porosity, deformations and residual stresses.

The range of application of friction stir welding of aluminum alloys widens [11, 12] due to its many advantages. Since the process is a solid-phase one, there are no problems of solidification, i.e., porosity, hot cracks and inclusions. Friction stir welding produces three different microstructural zones, namely, (1) a weld nugget (WN) zone, where the material undergoes considerable straining with stirring of the crystallites and heating and this yields a recrystallized structure with fine equiaxed grains [13 – 16], (2) a thermomechanically affected zone (TMAZ), where the material undergoes joint straining and heating but the temperature is insufficient for recrystallization, and (3) a heat-affected zone (HAZ), where the material is heated without mechanical straining. These zones differ in the structure and mechanical properties.

Many publications describe changes in the microstructure due to plastic straining and friction-induced heating as a result of friction stir welding [17 – 35]. The hardening precipitates in the weld zone have been reported to dissolve and coarsen in [17 – 19, 25, 31 – 35], and wide zones free of pre-

¹ Department of Mechanical Engineering, SRM University, Delhi NCR Campus, India (e-mail: gsrinu1882@gmail.com).

² Department of Mechanical Engineering, JNTUK, Kakinada, India.

³ Department of Mechanical Engineering, SSN College of Engineering, Chennai, India.

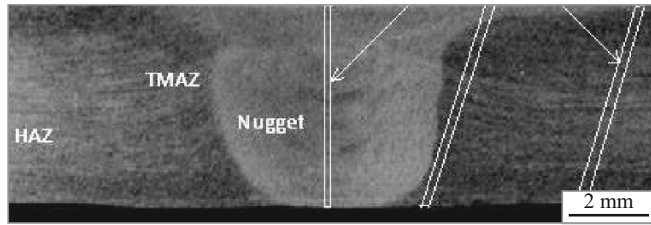


Fig. 1. Microstructure of the nugget zone of a weld with depicted places of cutting of specimens (indicated by the arrows) for transmission electron microscopy.

cipitates have been observed in [17, 19, 25, 33]. Mechanical fracture of welded joints may develop over the WNZ, TMAZ and HAZ depending on the introduced heat content determined by such parameters of the process as the stir speed and the feed [26–28]. The microstructure of a weld can also depend on the parameters of the welding process [29–31]. However, the data on friction stir welding of alloy 7020 of the Al–Zn–Mg system are quite scarce.

The aim of the present work was to study the effect of friction stir welding on the microstructure and mechanical properties of aluminum alloy 7020.

METHODS OF STUDY

The base material for the study was aluminum alloy AA7020 in the form of plates 4.5 mm thick. The alloy had the following chemical composition (in wt.%): 4.5 Zn, 1.45 Mg, 0.34 Fe, 0.28 Si, 0.22 Mn, 0.2 Cr, 0.059 Zr, 0.012 Ti, 0.002 Cu, the remainder Al.

We implemented welding with the help of a commercial friction stir unit. Billets $150 \times 110 \times 4.5$ mm in size were pressed densely to each other on the working table and subjected to friction stir butt welding. The tool for the friction stir welding was made of steel M2 (the Russian counterpart is R6M5). After several tests with different profiles of the head of the welding tool we found out that the best joining was provided by a threaded cone-shape head. The threaded head (left-handed metric thread with 1-mm step) had a length of 4.2 mm, and a diameter of 5 mm (on the side the holder) and 3 mm (at the tip of the head). The diameter of the holder was 15 mm. The speed of the tool was 1000 rpm, the speed of the welding was 200 mm/min, the slope of the tool was 1.50° .

The welded joints were cut in the transverse direction. The specimens for the metallographic study were prepared by the usual method. To uncover the microstructure, polished surfaces of the specimens were etched in Keller's reagent (5% HNO_3 , 2% HCl , 1% HF). The microstructure of various zones of the welded joints was studied with the help of a Leica DMLM optical microscope. The microhardness of the zones was determined using a Shimadzu Vickers microhardness tester at a load of 1 N with a hold of 15 sec. The tensile tests were performed according to ASTM E8 for transverse

specimens of welded joints and for the base metal of plates 4.5 mm thick. The plane bending tests of the joints were performed according to AWS B4. The specimens for the bending tests had a length of 152 mm and a width of 38 mm.

The specimens for transmission electron microscopy were cut from regions of WNZ, TMAZ and HAZ (Fig. 1) of an etched welded joint using an electric spark cutter. Each specimen was glued to a special wax used for the electron microscope study and polished to a thickness of about 100 μm . To avoid heating of the specimens, they were cut and polished in a running cooling liquid or in water. A disc 3 mm in diameter was cut by a special punch from the polished specimen and thinned mechanically. Ion etching was applied to both sides of the disc to form a depression that was deepened progressively to obtain a hole with thin edges transparent for electron beams. Such specimens were studied under a JEM-2100 electron microscope with an attachment for energy dispersive chemical analysis. The specimen holder in the microscope was made of beryllium to provide a double slope and a low background.

RESULTS AND DISCUSSION

Macro- and Microstructure

The macrostructure of a joint formed by friction stir welding is presented in Fig. 1. The nugget has an elliptic shape in the center and widens near the upper surface during the motion of the tool over the specimen in the welding process. It has been shown earlier in [36, 37] that a high speed of rotation of the tool renders the welding nugget elliptic. Figure 2 presents the microstructure in different zones of cross section of a welded joint. The structure of the base metal is represented by large grains stretched over the rolling direction and having a length of 150–200 μm and a width of 10–20 μm (Fig. 2a). In the TMAZ region (Fig. 2b) we can see that the grains flow toward the bottom side of the plate in accordance with the general direction of the flow of the metal under the action of the head of the tool. In the zone of the nugget the grain structure is different (Fig. 2b); the zone is fine-grained and equiaxed due to the recrystallization caused by plastic deformation and high temperature. The microstructure of the nugget is also presented in Fig. 2c. The grain size in the nugget is about 3–5 μm .

The results of the transmission electron microscopy of different zones of a weld of alloy AA7020-T6 are presented in Fig. 3. It can be seen (Fig. 3a) that the hardening precipitates in the base metal are a η -phase (MgZn_2) and a more stable ternary T -phase ($\text{Mg}_3\text{Zn}_3\text{Al}_2$). The size of these precipitates varies from 50 to 100 nm.

By the data of the analysis of the microstructure of the weld zone (Fig. 3b) almost all the hardening precipitates have dissolved. This means that the temperature in the nugget zone has been about 475°C , which is higher than the temperature of limited solubility and lower than the melting

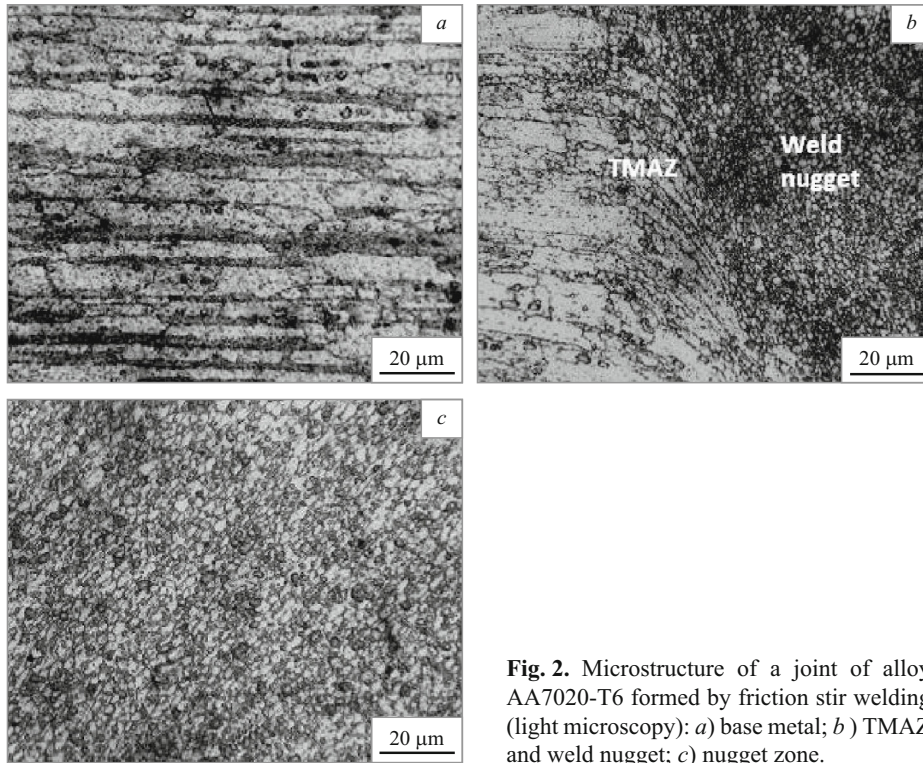


Fig. 2. Microstructure of a joint of alloy AA7020-T6 formed by friction stir welding (light microscopy): *a*) base metal; *b*) TMAZ and weld nugget; *c*) nugget zone.

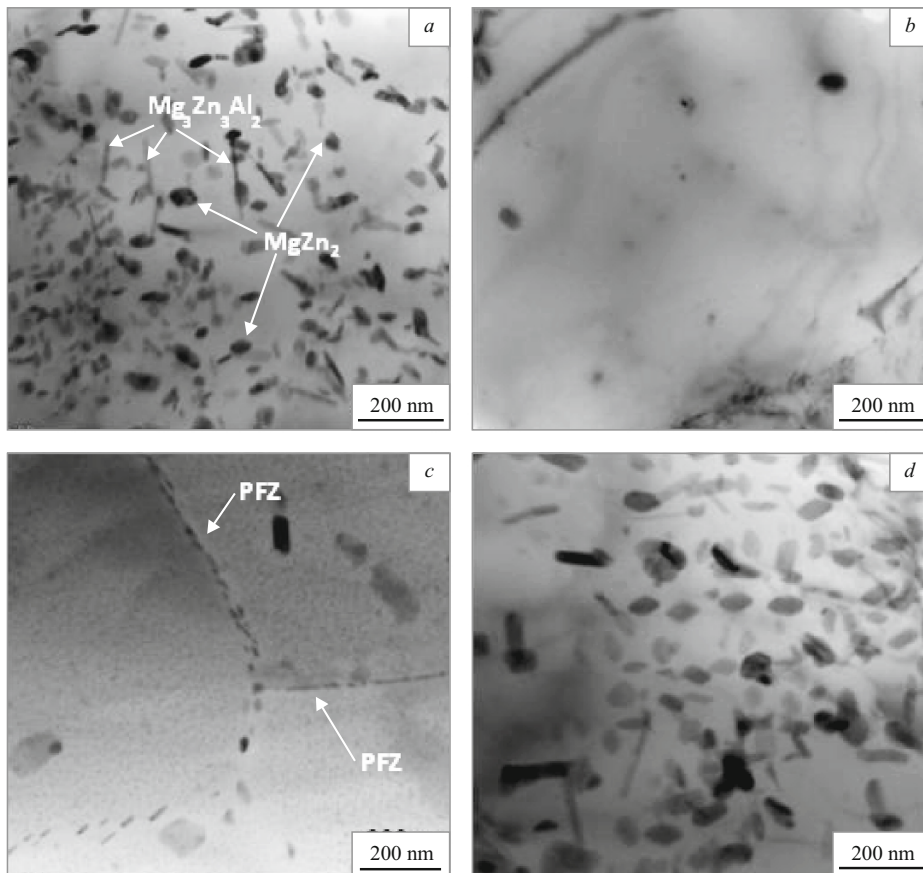


Fig. 3. Microstructure of a joint of alloy AA7020-T6 formed by friction stir welding (transmission electron microscopy): *a*) base metal; *b*) nugget zone; *c*) thermomechanically affected zone (PFZ are precipitate-free zones); *d*) heat-affected zone.

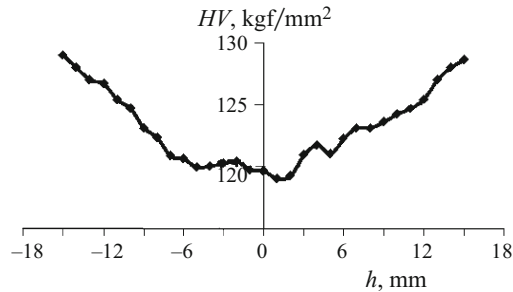


Fig. 4. Hardness profile of a welded joint in the transverse direction (h is the distance from the nugget).



Fig. 5. Appearance of fractured specimens after tensile tests.

point of the alloy [38, 39]. The microstructure of the TMAZ is presented in Fig. 3c. The hardening precipitates in it have also dissolved and formed again over grain boundaries. A zone free of precipitates has formed near grain boundaries. The morphology of the precipitates in the HAZ (Fig. 3d) is the same as in the base metal, but some precipitates have grown somewhat due to the thermal cycles in the HAZ during welding.

Mechanical Properties

The hardness profile in a welded joint is presented in Fig. 4. It can be seen that the hardness decreases gradually from a maximum value in the zone of the base metal to a minimum value in the nugget zone. The decrease in the hard-

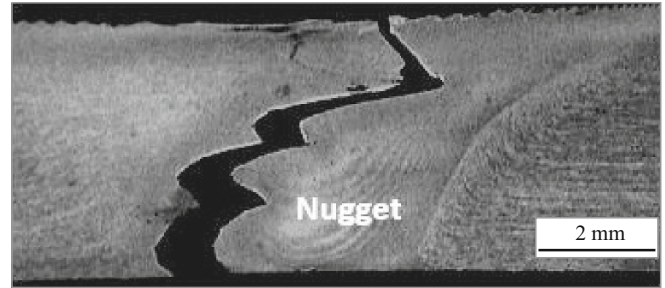


Fig. 6. Broken region of a specimen after a tensile test at the moment of failure.

ness is connected with dissolution of precipitates and elimination of strain hardening as a result of recrystallization. However, the refinement of grains in the nugget zone (by a factor of about 50 – 100) compensates considerably the loss in the hardness, which explains the high efficiency of these welded joints. The mean hardness in the nugget zone is 120 HV, i.e., is equal to about 88% of the hardness of the base metal (136 HV).

Table 1 presents the results of tensile tests of transverse specimens. The welded joints have a yield strength and an ultimate strength of 85 and 96% of the values of the base metal respectively. The elongation decreases inconsiderably. The tested specimens fracture over the nugget zone due to its softening. Figure 5 presents fractured specimens; Figure 6 presents formation of a crack. The trajectory of the crack is zigzag-like and long.

The bending tests were performed in a standard machine by a three-point scheme. The welded joints (Fig. 7) have a high ductility under plane bending by 180°, which is equal to the ductility of the base metal.

CONCLUSIONS

1. Alloy AA7020-T6 of the Al–Zn–Mg system exhibits good friction stir weldability. The yield strength of the welded joints amounts to 85% of that of the base metal.
2. Fracture under tensile tests occurs over the nugget zone of welds of AA7020-T6 due to softening of this zone caused by dissolution of the hardening particles.

TABLE 1. Mechanical Properties of a Welded Joint of Alloy AA7020-T6

Welding	$\sigma_{0.2}$, MPa	σ_r , MPa	δ , %	Localization of fracture
No welding (base metal)	310	372	14.0	–
Friction stir welding	263 (85%)	353 (95%)	12.0	Nugget zone
Argon arc welding [10]	214 (70%)	248 (66%)	6.2	–
Electron beam welding [9]	262 (84%)	343 (92%)	3.7	Fusion zone

Notes. 1. The values were averaged after three tests.

2. The parentheses contain the fraction of the corresponding characteristic of the base metal demonstrating the efficiency of the joint.

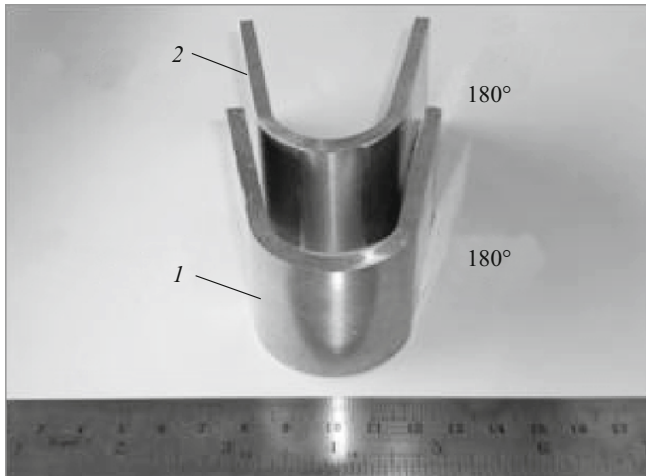


Fig. 7. Specimens of the base metal (1) and of welded joint (2) after bending tests.

3. The ductility due to bending of the weld by 180° does not differ from that of the base metal.

4. By the data of transmission electron microscopy all the hardening precipitates dissolve in the nugget zone and in the thermomechanically affected zone of welded joints of alloy AA7020-T6. In the heat-affected zone most of the precipitates are preserved.

5. Regions free of precipitates form in the thermomechanically affected zone of welds of alloy AA7020-T6 due to their dissolution and repeated precipitation over grain boundaries.

The authors are grateful to Dr. G. Madhusudhan Reddy, Scientist of the Defense Metallurgical Research Laboratory (DMRL) of Hyderabad, for providing the facility for carrying out the present study.

REFERENCES

1. P. K. Ghosh, S. R. Gupta, P. C. Gupta, and R. Rathi, "Fatigue characteristics of pulsed MIG welded Al-Zn-Mg alloy," *J. Mater. Sci.*, **26**, 6161 – 6170 (1991).
2. I. B. Robinson and F. R. Baysinger, "Welding aluminum alloys 7039," *Welding J.*, **45**, 433s – 444s (1966).
3. Abhay K. Jha, Ramesh Narayanan, P. Diwakar, et al., "Metallurgical analysis of cracked aluminum alloy AFNOR 7020 components used in satellite launch vehicles," *Eng. Failure Analysis J.*, **11**, 463 – 474 (2004).
4. K. Diwakar Jha Abhay, V. Sreekumar, K. M. C. Mittal, "Cracking of AFNOR 7020 aluminum alloy component: a metallurgical investigation," *Eng. Failure Analysis J.*, **13**, 1233 – 1239 (2006).
5. T. Ma and G. Den Ouden, "Heat affected zone softening during arc welding of Al-Zn-Mg alloys," *Int. J. Joining Mater.*, **8**(10), 105 – 110 (1996).
6. L. F. Mondolfo, "Aluminum alloys, structure and properties," *Met. Mater.*, **5**(10), 95 – 124 (1971).
7. S. Kou and Y. Le, "Nucleation mechanisms and grain refining of weld metal," *Welding J.*, **79**(1), 9s – 17s (2000).
8. Ch. Lee, S. Kim, and W. E. P. Yoon, "Electron beam welding characteristics of high strength aluminum alloys for express train applications," *Sci. Technol. Weld. Joining*, **5**(5), 277 – 283 (2000).
9. G. Cam and M. Kocak, "Microstructural and mechanical characterization of electron beam welded Al-alloy 7020," *J. Mater. Sci.*, **42**, 7154 – 7161 (2007).
10. Janaki Ram, G. D. Mitra, T. K. Shankar, and V. S. Sundaresan, "Microstructural refinement through inoculation of type 7020 Al-Zn-Mg alloy welds and its effect on hot cracking and tensile properties," *J. Mater. Proc. Technol.*, **142**, 174 – 181 (2003).
11. W. M. Nicholas, E. D. Needman, et al., *Patent Appl. No. 9125978.8 (Dec. 1991) and US Patent No. 5460317 (Oct. 1995)*.
12. C. Dawes and W. Thomas, *TWI Bull.*, Vol. 6, Nov./Dec., 124 (1995).
13. C. G. Rhodes, M. W. Mahoney, W. H. Bingel, et al., "Effects of friction stir welding on microstructure of 7075 aluminum," *Scr. Mater.*, **36**, 69 – 75 (1997).
14. G. Liu, L. E. Murr, C. S. Niou, et al., "Microstructural aspects of the friction stir welding of 6061-T6 aluminum," *Scr. Mater.*, **37**, 355 (1997).
15. K. V. Jata and S. L. Semiatin, "Continuous dynamic recrystallization during friction stir welding of high strength aluminum alloys," *Scr. Mater.*, **43**(8), 743 – 749 (2000).
16. S. Benavides, Y. Li, L. E. Murr, et al., "Low-temperature friction-stir-welding of 2024 aluminum," *Scr. Mater.*, **41**(8), 809 – 815 (1999), doi: 10.1016/S1359-6462(99)00226-2.
17. K. A. A. Hassan Prangnell, P. B. Norman, et al., *Sci. Technol. Weld. JOI*, **8**, 257 – 268 (2003).
18. J. Q. Su, T. W. Nelson, R. Mishra, and M. Mahoney, *Acta Mater.*, **51**, 713 – 729 (2003).
19. C. G. Rhodes, M. W. Mahoney, W. H. Bingel, et al., *Scr. Mater.*, **36**, 69 – 75 (1997).
20. K. V. Jata, K. K. Sankaran, and J. J. Ruschau, *Metall. Mater. Trans.*, **31A**, 2181 – 2192 (2000).
21. G. Liu, L. E. Murr, C. S. Niou, et al., *Scr. Mater.*, **37**, 355 – 361 (1997).
22. Y. S. Sato, H. Kokawa, M. Enomoto, et al., *Metall. Mater. Trans.*, **30A**, 3125 – 3130 (1999).
23. Y. S. Sato, H. Kokawa, M. Enomoto, and S. Jogan, *Metall. Mater. Trans.*, **30A**, 2429 – 2437 (1999).
24. K. V. Jata and S. L. Semiatin, *Scr. Mater.*, **43**, 743 – 749 (2000).
25. S. Benavides, Y. Li, L. E. Murr, et al., *Scr. Mater.*, **41**, 809 – 815 (1999).
26. M. W. Mahoney, C. G. Rhodes, J. G. Flintoff, et al., *Metall. Mater. Trans.*, **29A**, 1955 – 1964 (1998).
27. M. Peel, A. Steuwer, M. Preuss, and P. J. Withers, *Acta Mater.*, **51**, 4791 – 4801 (2003).
28. A. P. Reynolds, W. D. Lockwood, and T. U. Seidel, *Mater. Sci. Forum*, **331 – 337**, 1719 – 1724 (2000).
29. H. J. Liu, H. Fujii, M. Maeda, and K. Nogi, *J. Mater. Proc. Technol.*, **142**, 692 – 696 (2003).
30. B. Yang, I. Yan, M. A. Sutton, and A. P. Reynolds, *Mater. Sci. Eng. A-Struct.*, **364**, 55 – 65 (2004).
31. K. A. A. Hassan, A. F. Norman, and P. B. Prangnell, *Mater. Sci. Forum*, **396 – 400**, 1549 – 1554 (2002).
32. K. A. A. Hassan, A. F. Norman, and P. B. Prangnell, "The effect of welding conditions on the microstructure and mechanical properties of the nugget zone in AA7010 alloy friction stir welds," in: *3rd Int. Symp. on Friction Stir Welding*, Kobe, Japan (2001).
33. K. V. Jata, *Mater. Sci. Forum*, **331 – 337**, 1701 – 1712 (2000).

34. K. A. A. Hassan, A. F. Norman, A. F. Price, and P. B. Prangnell, *Acta Mater.*, **51**, 1923 – 1936 (2003).
35. J. D. Robinson, A. Sullivan, H. R. Shercliff, and G. Mcshane, “Microstructural evolution during friction stir welding of AA7449,” in: *5th Int. Friction Stir Welding Symposium*, Metz, France (2004).
36. C. G. Rodes, M. W. Mahoney, W. H. Bingel, et al., “Effects of friction stir welding on microstructure of 7075 aluminum,” *Scr. Mater.*, **36**, 69 – 75 (1997).
37. M. W. Mahoney, C. G. Rodes, J. G. Flintoff, et al., “Properties of friction stir-welded 7075 T651 aluminum,” *Metall. Mater. Trans.*, **29A**, 1955 – 1964 (1998).
38. K. A. A. Hassan, P. B. Prangnell, A. F. Norman, et al., *Sci. Technol. Weld. Joining*, **8**(4), 257 – 268 (2003).
39. Y. Sato, H. Kokawa, M. Enomoto, and S. Jogan, “Microstructural evaluation of 6063 aluminum during friction stir welding,” *Metall. Mater. Trans.*, **30A**, 2429 – 2437 (1999).